

Analysis of Structural Distortions in Non-Stoichiometric Ternary Platinum Oxides: $\text{Li}_{0.64}\text{Pt}_3\text{O}_4$ and $\text{Co}_{0.37}\text{Na}_{0.14}\text{Pt}_3\text{O}_4$

BY K. B. SCHWARTZ, J. B. PARISE AND C. T. PREWITT

*Department of Earth and Space Sciences, State University of New York at Stony Brook, Stony Brook,
New York 11794, USA*

AND R. D. SHANNON

Central Research and Development Department, E.I. du Pont de Nemours and Company, Wilmington,
Delaware 19898, USA*

(Received 20 November 1981; accepted 5 March 1982)

Abstract

The structures of $\text{Li}_{0.64}\text{Pt}_3\text{O}_4$ and $\text{Co}_{0.37}\text{Na}_{0.14}\text{Pt}_3\text{O}_4$ have been determined from neutron powder diffraction experiments and found to exhibit two kinds of internal structural distortions distinguishing them from the prototype NaPt_3O_4 structure in which the Na counterion occupies eight-coordinated cubic sites in the PtO_4 framework. Both the $\text{Li}_{0.64}\text{Pt}_3\text{O}_4$ and $\text{Co}_{0.37}\text{Na}_{0.14}\text{Pt}_3\text{O}_4$ structures were characterized by modifications to the geometry of the eight-coordinated counterion site. In $\text{Li}_{0.64}\text{Pt}_3\text{O}_4$ the Li ions were randomly distributed on these sites, and the oxygen coordination was no longer cubic, with four short Li–O distances of 2.22 Å and four long ones of 2.65 Å in the configuration of two interpenetrating tetrahedra. In $\text{Co}_{0.37}\text{Na}_{0.14}\text{Pt}_3\text{O}_4$ there was ordering of Co, Na, and vacancies in the eight-coordinated sites, which imposed a structural limit on substitution of eight-coordinated atoms to 0.5 per formula unit. In this case, cation–oxygen coordination was cubic, with eight O atoms at a distance of 2.36 (1) Å from the occupied counterion site. The $\text{Li}_{0.64}\text{Pt}_3\text{O}_4$ structure, with $a = 5.6242$ (2) Å and $Z = 2$, was refined in space group $P\bar{4}3n$ by the Rietveld profile technique with a final weighted profile discrepancy factor $R_{wp} = 0.160$ for 35 reflections collected at $\lambda = 1.343$ Å. The $\text{Co}_{0.37}\text{Na}_{0.14}\text{Pt}_3\text{O}_4$ structure, with $a = 5.6321$ (4) Å and $Z = 2$, was refined in space group $Pm\bar{3}$ using integrated intensities with a final weighted $R_w = 0.036$ for 15 observations representing 22 reflections collected at $\lambda = 2.460$ Å.

1. Introduction

In light of their application as chlor-alkali anodes and H_2O_2 fuel-cell electrocatalysts, ternary platinum oxides

of the type $M_x\text{Pt}_3\text{O}_4$ are of considerable technological interest (Shannon, Gier, Carcia, Bierstedt, Flippen & Vega, 1982, and references within). A wide range of compositions, with counterions $M = \text{Na}, \text{Li}, \text{K}, \text{Mg}, \text{Ca}, \text{Sr}, \text{Ba}, \text{Co}, \text{Ni}, \text{Zn}$ and Cd , have been reported (Bergner & Kohlhaas, 1973; Cahen, Ibers & Mueller, 1974; Cahen, Ibers & Wagner, 1974; Lazarev & Shaplygin, 1978*a,b,c*; Shannon *et al.*, 1982). The bulk of this work has concentrated on the methods of synthesis, thermal stability, and physical properties of these compounds. For the most part, $M_x\text{Pt}_3\text{O}_4$ compositions have been poorly defined with respect to both stoichiometry and the response of the $M_x\text{Pt}_3\text{O}_4$ structure to partial counterion occupancies and wide variations in the size of the metal cations present.

All $M_x\text{Pt}_3\text{O}_4$ compositions have been reported to have the NaPt_3O_4 structure (Waser & McClanahan, 1951), which consists of infinite stacks of parallel square-planar PtO_4 groups extending along all three crystallographic axes. The counterion resides in an eight-coordinated cubic polyhedron that separates the PtO_4 groups in each direction (Fig. 1). A neutron powder diffraction study of $\text{Na}_{1.0}\text{Pt}_3\text{O}_4$ and $\text{Na}_{0.73}\text{Pt}_3\text{O}_4$ (Schwartz, Prewitt, Shannon, Corliss, Hastings & Chamberland, 1982) has confirmed this cubic structure (space group $Pm\bar{3}n$) and demonstrated

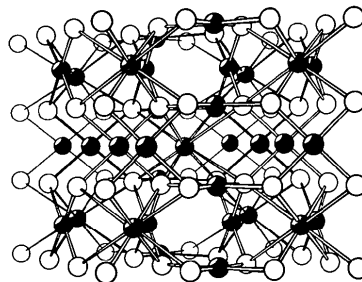


Fig. 1. Ideal $M\text{Pt}_3\text{O}_4$ structure, space group $Pm\bar{3}n$ (after Schwartz *et al.*, 1982).

* Contribution No. 2980.

its ability to respond to significant vacancies in the counterion site by unit-cell contraction with no long-range structural distortions.

The presence of cobalt and lithium as major counterion components in $M_x\text{Pt}_3\text{O}_4$ compounds is of particular interest because of their smaller size. Whereas Na^+ has an ionic radius (IR) of 1.18 Å in eightfold coordination (Shannon, 1976), eight-coordinated Li^+ ($IR = 0.92$ Å) and Co^{2+} ($IR = 0.90$ Å) are quite small for this site. Eight coordination is uncommon for transition metals with d^3 – d^{10} electron configurations such as cobalt (Burdett, Hoffmann & Fay, 1978), and rare for lithium as well. Given this situation, the potential for internal structural deformations of the ideal NaPt_3O_4 structure for these compositions clearly exists.

This paper describes a study of the structure and crystal chemistry of $\text{Li}_{0.64}\text{Pt}_3\text{O}_4$ and $\text{Co}_{0.37}\text{Na}_{0.14}\text{Pt}_3\text{O}_4$ and discusses the possible structure of a poorly defined $\text{Ni}_x\text{Na}_y\text{Pt}_3\text{O}_4$ composition ($x \sim 0.4$, $y \sim 0.2$). These compositions were chosen for their tendencies to be strongly non-stoichiometric (Shannon *et al.*, 1982) and because they contained some of the smaller counterions known to substitute in the $M_x\text{Pt}_3\text{O}_4$ structure. Structure determinations and refinements were made by use of neutron powder diffraction data. Atomic absorption analysis was employed to determine counterion content and provided an important chemical constraint during the refinement procedure.

2. Experimental

Polycrystalline $\text{Li}_{0.64}\text{Pt}_3\text{O}_4$ was prepared by solid-state reaction of reagent grade LiF , LiNO_3 and $\alpha\text{-PtO}_2$ in a molar ratio of 1:1:6. The 16.85 g mixture was ground vigorously, pressed into pellets in a 1" die at 4500 lbs (2.54 cm die at 2041 kg) and heated slowly (~ 15 K h^{-1}) under atmospheric conditions to 823 K in a covered Al_2O_3 crucible. After being held at this temperature for 4 h, the material was quenched in air to room temperature. It was then reground and pelletized and heated slowly to 873 K where it was held for 14 h and then quenched. The resulting fine-grained black powder was boiled twice in *aqua regia* and washed thoroughly with distilled water before any analysis. Similar syntheses were performed for $\text{Co}_{0.37}\text{Na}_{0.14}\text{Pt}_3\text{O}_4$ using a 22.20 g mixture of reagent grade NaF , $\text{Co}(\text{NO}_3)_2 \cdot 6\text{H}_2\text{O}$, CoF_2 and $\alpha\text{-PtO}_2$ in a 1:1:2:12 molar ratio and $\text{Ni}_x\text{Na}_y\text{Pt}_3\text{O}_4$ using a 28.13 g mixture of reagent grade NaF , NiF_2 , $\text{Ni}(\text{NO}_3)_2 \cdot 6\text{H}_2\text{O}$ and $\alpha\text{-PtO}_2$ in a 1:1:2:12 molar ratio. The presence of NaF was necessitated in the preparation of $\text{Co}_{0.37}\text{Na}_{0.14}\text{Pt}_3\text{O}_4$ because of the instability of pure Na -free $\text{Co}_x\text{Pt}_3\text{O}_4$.

Unit-cell dimensions were determined for the three samples by least-squares refinement using data

from X-ray powder diffraction patterns obtained with a Guinier–Hägg focusing camera (radius = 40 mm) using monochromatic $\text{Cu } K\alpha_1$ radiation ($\lambda = 1.5405$ Å) and an internal standard of Si ($a = 5.4305$ Å). Line positions on the film were determined to ± 5 μm with a Mann film reader. The values obtained were: $a = 5.6242$ (2) Å for $\text{Li}_{0.64}\text{Pt}_3\text{O}_4$, $a = 5.6321$ (4) Å for $\text{Co}_{0.37}\text{Na}_{0.14}\text{Pt}_3\text{O}_4$, and $a = 5.6256$ (5) Å for $\text{Ni}_x\text{Na}_y\text{Pt}_3\text{O}_4$. No impurity phases were detected in any of the samples in the X-ray analysis.

The actual lithium content, 0.64 (11) cations per formula unit, was determined by atomic absorption analysis in triplicate. Counterion contents for cobalt, 0.37 (2) cations per formula unit, and sodium, 0.14 (1) cations per formula unit, were determined by quintuplicate atomic absorption analysis. The materials were dissolved in HBr for the analyses.

Neutron powder diffraction experiments were performed at room temperature on two powder diffractometers at the High-Flux-Beam Reactor of Brookhaven National Laboratory. The samples were pressed into cylindrical pellets approximately 1 cm in diameter and 2 cm in length and placed in the neutron beam with no holder in order to maximize the signal-to-background ratio and avoid extraneous peaks. Data were collected at wavelengths of 1.343 and 2.460 Å for each sample. Experimental conditions for all data sets are given in Table 1. The 100 reflection for $\text{Co}_{0.37}\text{Na}_{0.14}\text{Pt}_3\text{O}_4$ ($2\theta = 10$ to 14.95°) was collected ten times at 1.343 Å and averaged in order to increase the precision of intensity determination for this peak. Transmission factors were measured at 2.460 Å in order to apply an absorption correction as described by Hewat (1979), and μr was found to be 0.57 for $\text{Li}_{0.64}\text{Pt}_3\text{O}_4$ and 0.39 for $\text{Co}_{0.37}\text{Na}_{0.14}\text{Pt}_3\text{O}_4$, where μ is the linear absorption coefficient and r is the radius of the cylindrical sample.

Table 1. *Experimental conditions*

Wavelength: 1.343 Å Monochromator: Ge (111) Analyser: pyrolytic graphite (004)			
	$\text{Li}_{0.64}\text{Pt}_3\text{O}_4$	$\text{Co}_{0.37}\text{Na}_{0.14}\text{Pt}_3\text{O}_4$	
2θ range	15.00–112.00°	10.00–125.00°*	
Step width	0.05° 2θ	0.05° 2θ	
Counting time	133.3 s step^{-1}	160 s step^{-1}	
Ref./peaks†	35/28	99/48	
Wavelength: 2.460 Å Monochromator: pyrolytic graphite (002) Analyser: pyrolytic graphite (004)			
	$\text{Li}_{0.64}\text{Pt}_3\text{O}_4$	$\text{Co}_{0.37}\text{Na}_{0.14}\text{Pt}_3\text{O}_4$	$\text{Ni}_x\text{Na}_y\text{Pt}_3\text{O}_4$
2θ range	22.00–134.00°	15.00–130.00°	15.00–130.00°
Step width	0.05° 2θ	0.10° 2θ	0.10° 2θ
Counting time	49 s step^{-1}	51 s step^{-1}	102 s step^{-1}
Ref./peaks	10/10	22/15	22/15

* The 2θ range 10.00–15.00° was collected ten times and averaged for this sample (see text).

† Number of reflections/number of peaks.

Structure refinements were performed using the method of profile analysis with the program *PROFILE* written by Rietveld (1969*a, b*) and modified by Hewat (1973). The neutron scattering amplitudes used were: $b(\text{Na}) = 3.60$, $b(\text{Li}) = -2.03$, $b(\text{Co}) = 2.80$, $b(\text{Ni}) = 10.3$, $b(\text{Pt}) = 9.5$, and $b(\text{O}) = 5.800$ fm (Bacon, 1978; Koester, 1977). The structures were also refined with integrated intensities based upon stepwise summation of the raw data collected at 2.460 Å with a background correction using the program *POWLS* (Will, 1979). *POWLS* (powder least squares) performs structure refinement by least-squares analysis through minimization of the function $\sum w(I_{\text{obs}}^2 - I_{\text{calc}}^2)^2$, where I_{obs} may be a single reflection or a group of unresolved reflections in the powder diffraction diagram. I_{calc} corresponds to the summation over all overlapping reflections contributing to an observation. w denotes the weight based upon estimated standard deviations of the observed intensities.

Discrepancy factors for structure refinements using *PROFILE* are defined as $R_I = \sum |I_{\text{obs}} - I_{\text{calc}}| / \sum I_{\text{obs}}$ for integrated intensities determined by the approximation given by Rietveld (1969*a, b*), and $R_{wP} = [\sum w(Y_{\text{obs}} - Y_{\text{calc}})^2 / \sum w(Y_{\text{obs}})^2]^{1/2}$ for weighted point-by-point intensities. The expected discrepancy factor $R_E = \{(N - P + C) / \sum w(Y_{\text{obs}})^2\}^{1/2}$, where $N - P + C$ is the number of degrees of freedom (Rietveld, 1969*a, b*; Hewat, 1973). Y represents counts per step corrected for background and w is a statistical weight $1/\sigma^2 = 1/Y$. For *POWLS* integrated intensity refinements, $R = \sum |I_{\text{obs}} - I_{\text{calc}}| / \sum I_{\text{obs}}$ and $R_w = [\sum w(I_{\text{obs}} - I_{\text{calc}})^2 / \sum w(I_{\text{obs}})^2]^{1/2}$, where the weighting factor $w = 1/\sigma^2$. The goodness-of-fit $\chi^2 = [\sum w(I_{\text{obs}} - I_{\text{calc}})^2 / (N - P + C)]^{1/2}$.

3. Results

3.1. Structure refinement of $\text{Li}_{0.64}\text{Pt}_3\text{O}_4$

Examination of the neutron powder diffraction pattern for $\text{Li}_{0.64}\text{Pt}_3\text{O}_4$ indicates the same systematic absences observed for the NaPt_3O_4 sample, *i.e.* $hkl: l \neq 2n$. However, attempts to refine the structure of $\text{Li}_{0.64}\text{Pt}_3\text{O}_4$ in space group *Pm3n* proved unsatisfactory. The discrepancy factors were $R_I = 0.127$ and $R_{wP} = 0.244$, with $R_E = 0.123$. Cahen, Ibers & Shannon (1972), in a single-crystal X-ray diffraction structure refinement, have suggested that $\text{Ni}_{0.25}\text{Pt}_3\text{O}_4$ may crystallize in space group *P43n*, a non-centrosymmetric subgroup of *Pm3n*. Refinement of the structure of $\text{Li}_{0.64}\text{Pt}_3\text{O}_4$ in this space group reduces R_{wP} to 0.165 with the addition of one parameter. Individual isotropic temperature factors are used for these refinements. Unlike NaPt_3O_4 , the oxygen position for $\text{Li}_{0.64}\text{Pt}_3\text{O}_4$ is not constrained at $\frac{1}{4}, \frac{1}{4}, \frac{1}{4}$ but is free to move along the body diagonal of the cubic unit cell at position x, x, x .

Table 2. Structure refinements for $\text{Li}_{0.64}\text{Pt}_3\text{O}_4$ (cubic, *P43n*) using neutron powder diffraction data

	x	y	z	
Li	2(a)	0	0	0
Pt	6(d)	$\frac{1}{4}$	0	$\frac{1}{4}$
O	8(e)	x	x	x
				$\beta_{11} = \beta_{22} = \beta_{33}$ $\beta_{12} = \beta_{13} = \beta_{23}$
	(I)	(II)	(III)	
	$\lambda = 1.343$ Å	$\lambda = 2.460$ Å	$\lambda = 2.460$ Å	
	<i>PROFILE</i>	<i>PROFILE</i>	<i>POWLS</i>	
Occupancy: Li	0.64	0.64	0.64	
Occupancy: Pt	3.00	3.00	3.00	
x : O	0.2717 (3)*	0.2722 (5)	0.271 (1)	
B : Li	2.1 (4)†			
B : Pt	0.16 (2)†	B : overall	-0.06 (9)‡	-0.2 (4)‡
B : O	0.82 (3)§			
β_{11} : O	0.0065 (4)	-	-	
β_{12} : O	0.0037 (7)	-	-	
B_{11} : O	0.83 (5)¶	-	-	
B_{12} : O	0.46 (9)¶	-	-	
R_I	0.037	0.046	χ^2 2.16	
R_{wP}	0.160	0.169	R 0.040	
R_E	0.123	0.070	R_w 0.057	

* Errors in parentheses.

† Individual isotropic temperature factor in Å² as refined.

‡ Overall isotropic temperature factor in Å² as refined, corrected for absorption by 0.43 Å² (see text).

§ Equivalent isotropic temperature factor in Å² calculated from anisotropic temperature-factor coefficients.

|| Anisotropic temperature-factor coefficients used during refinement of the form: $\exp[-(\beta_{11}h^2 + \beta_{22}k^2 + \beta_{33}l^2 + 2\beta_{12}hk + 2\beta_{13}hl + 2\beta_{23}kl)]$.

¶ Elements of the mean-square displacement matrix B , where $B_{ij} = 8\pi\langle\mu^2\rangle$, $\langle\mu^2\rangle$ being the mean-square displacement from equilibrium position in Å².

Structure refinements for $\text{Li}_{0.64}\text{Pt}_3\text{O}_4$ using neutron powder diffraction data are given in Table 2. The data collected at 1.343 Å include 35 independent reflections and the data collected at 2.460 Å include 10 independent reflections.* The refined values for the oxygen position obtained from these three refinements all agree within one standard deviation, a significant demonstration that consistent structural information can be derived from data collected on different diffractometers at different wavelengths and refined by different methods. The oxygen positional parameter, $x = 0.272$, corresponds to distortion of the eight-coordinated lithium site from the perfect cube in NaPt_3O_4 . The nature of this distortion is discussed later.

In these refinements the lithium occupancy is constrained to the chemically analyzed value, 0.64 cations per formula unit, and the platinum site is assumed to be fully occupied. Refinement of the

* A list of observed and calculated intensities has been deposited with the British Library Lending Division as Supplementary Publication No. SUP 36821 (4 pp.). Copies may be obtained through The Executive Secretary, International Union of Crystallography, 5 Abbey Square, Chester CH1 2HU, England.

scattering length of the lithium site, which yields a lithium occupancy of 0.71 (5) cations per formula unit using the 1.343 Å data, does not affect any other refined parameters nor does it significantly lower the discrepancy factors.

For the final stages of structure refinement with the short-wavelength data, anisotropic temperature factors are used for oxygen. This refinement introduces one additional parameter and leads to a decrease in R_{wp} from 0.165 to 0.160 and a decrease in R_I from 0.050 to 0.037. For refinements using the long-wavelength data a single overall thermal parameter, corrected for the effect of absorption by 0.43 Å², is employed. This correction is applied at the conclusion of the refinement procedure as described by Hewat (1979). Since the Debye–Waller correction factor $\Delta B \propto \lambda^2$ and $\mu \propto \lambda$, the absorption correction is reduced by almost an order of magnitude for the refinements using short-wavelength data and is therefore disregarded. The thermal parameters refined with long-wavelength data are not well defined because of the scantiness of the data, particularly the lack of data above $\sin \theta/\lambda = 0.37 \text{ \AA}^{-1}$.

3.2. Structure refinement of $\text{Co}_{0.37}\text{Na}_{0.14}\text{Pt}_3\text{O}_4$

In contrast to $\text{Li}_{0.64}\text{Pt}_3\text{O}_4$, weak reflections of the type hhl : $l \neq 2n$ are observed in the neutron powder diffraction pattern of $\text{Co}_{0.37}\text{Na}_{0.14}\text{Pt}_3\text{O}_4$. These reflections should be systematically absent for space groups $Pm3n$ and $P43n$, and leaves the diffraction pattern for $\text{Co}_{0.37}\text{Na}_{0.14}\text{Pt}_3\text{O}_4$ with no systematic absences. This suggests that $\text{Co}_{0.37}\text{Na}_{0.14}\text{Pt}_3\text{O}_4$ crystallizes in space group $Pm3$ or $P23$. These two subgroups of $Pm3n$ are characterized by inequivalent positions at 0,0,0 (*A*) and $\frac{1}{2}, \frac{1}{2}, \frac{1}{2}$ (*B*), which indicates ordering on the eight-coordinated sites. However, refinements attempted in the non-centrosymmetric space group $P23$ would not converge.

The results of structure refinements for $\text{Co}_{0.37}\text{Na}_{0.14}\text{Pt}_3\text{O}_4$ in the centrosymmetric space group $Pm3$, using neutron powder diffraction data collected at 1.343 and 2.460 Å, by the profile and integrated intensity methods are given in Table 3. The short-wavelength data include 99 independent reflections and the long-wavelength data include 15 observations representing 22 reflections.* The agreement of structural parameters obtained from the various refinements is again good. The oxygen position is still constrained to remain on the threefold axis at position x, x, x as in $\text{Li}_{0.64}\text{Pt}_3\text{O}_4$ and the x positional parameter for the platinum site is now also free to vary from $\frac{1}{4}$ at $x, 0, \frac{1}{2}$. Because of the more complex crystal chemistry of this sample, an overall isotropic metal temperature factor is used. The two anisotropic temperature factor coeffi-

Table 3. Structure refinements for $\text{Co}_{0.37}\text{Na}_{0.14}\text{Pt}_3\text{O}_4$ (cubic, $Pm3$) using neutron powder diffraction data

	<i>x</i>	<i>y</i>	<i>z</i>			
<i>A</i>	1(<i>a</i>)	0	0	0		
<i>B</i>	1(<i>b</i>)	$\frac{1}{2}$	$\frac{1}{2}$	$\frac{1}{2}$		
Pt	6(<i>f</i>)	<i>x</i>	0	$\frac{1}{2}$		
O	8(<i>i</i>)	<i>x</i>	<i>x</i>	<i>x</i>	$\beta_{11} = \beta_{22} = \beta_{33}$	$\beta_{12} = \beta_{13} = \beta_{23}$
					(I)	(II)
					$\lambda = 1.343 \text{ \AA}$	$\lambda = 2.460 \text{ \AA}$
					PROFILE	PROFILE
						POWLS
Scattering: <i>A</i> *					1.9 (2)	2.1 (3)
Scattering: <i>B</i> *					1.2 (2)	1.0 (3)
Scattering: Pt*					57	57
<i>x</i> : Pt					0.251 (1)	0.253 (3)
<i>x</i> : O					0.2425 (8)	0.242 (2)
<i>B</i> : metal					0.24 (2)†	0.7 (2)†
<i>B</i> : O					1.00 (3)‡	1.1 (2)†
β_{11} : O					0.0079 (4)	—
β_{12} : O					0.0045 (4)	—
R_I					0.060	0.052
R_{wp}					0.155	0.174
R_E					0.110	0.052
						χ^2 0.82
						R_w 0.026
						R_w 0.036

* Site scattering length per unit cell in fm (see text).

† Isotropic temperature factor in Å² as refined with $\lambda = 2.460 \text{ \AA}$ values corrected for absorption by 0.22 Å² (see text).

‡ Equivalent isotropic temperature factor in Å² calculated from anisotropic temperature-factor coefficients.

icients for the O atom are included for the short-wavelength data, and only isotropic temperature factors are used in refinements using long-wavelength data. Thermal parameters obtained from the 2.460 Å data are corrected for absorption by 0.22 Å².

Occupancy factors for the cation sites in this ordered, non-stoichiometric compound are represented by values of site scattering per unit cell given in fm, which correspond to the sums of the product of the site occupancy (*n*) and the neutron scattering length (*b*) for each atom in each site (i.e. $\sum b_i n_i$). The refined values therefore contain information on the degree of occupancy of each cation site and the type of cation which occupies each site. When the sums of the scattering lengths of the two counterion sites are constrained to 3.1 fm per unit cell, the value corresponding to the total Co + Na as determined by wet chemistry, the refined scattering length for the *B* site is 40–65% smaller than that for the *A* site, regardless of which data set or refinement program is used.

A comparison of the observed integrated intensities of the ordering reflections for long-wavelength data generated by PROFILE with those measured for POWLS reveals that the PROFILE intensities are systematically lower than those measured for POWLS. In PROFILE, a Gaussian peak shape is assumed, and all intensity within 1.5 calculated peak widths on either side of the peak position is included in the refinement, an assumption that is normally valid and in the

* See previous footnote.

present case quite adequate for the determination of the intensities of the major reflections. However, it is apparent from the pattern (e.g. Fig. 2) that the weak peaks have a significant portion of their intensity outside this region due to line broadening. These diffuse reflections indicate some degree of short-range order between metal atoms and vacancies.

For calculation of peak intensities for use in *POWLS*, it was possible to measure the intensity of the reflections more accurately. For example, the 100 reflection was measured from $2\theta = 23.00$ to 26.90° for *POWLS*, but only the range $2\theta = 24.31$ to 26.31° was taken in *PROFILE*. It is therefore felt that the intensities used in the *POWLS* refinement are more reliable in this case. Since the refined values of scattering for the *A* and *B* sites are most strongly dependent on the intensity of the weak ordering reflections, the site scattering information derived from the *POWLS* refinement is preferred over the ordering model of the *PROFILE* refinements. There are no other statistically significant differences in structural parameters between the different refinements.

The use of a constraint on the sum of the scattering lengths of the two counterion sites assumes that all the Co + Na cations are in eightfold coordination and the square-planar site is fully occupied by platinum. In order to examine the possibility of square-planar cobalt, a structure refinement was performed with integrated intensities with one additional variable parameter, the scattering length of the square-planar site. For this refinement the total Co + Na content was still constrained to the chemically analyzed value, but Co was also allowed to be present in the platinum site with the additional constraint that $(\text{Co} + \text{Pt})^{\text{IV}} = 3.00$ cations per formula unit. This refinement resulted in a decrease for R_w from 0.088 to 0.036 and a decrease in the goodness-of-fit from 1.87 to 0.82. It is the results of this refinement that are reported in Table 3. The crystal-chemical implications of these final refined

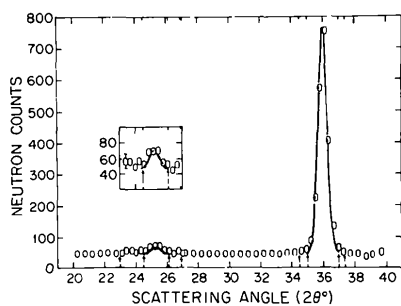


Fig. 2. Neutron powder diffraction pattern for $\text{Co}_{0.37}\text{Na}_{0.14}\text{Pt}_3\text{O}_4$ at 2.460 \AA showing 100 and 110 reflections. Open circles are observed intensities and solid lines are the *PROFILE* calculated fit. For each reflection the inner set of arrows is the 2θ range included by *PROFILE* and the outer set of arrows is the 2θ range included for integrated intensity determination for use in *POWLS*.

values for the cation-site scattering lengths and the nature of the internal structural deformations for $\text{Co}_{0.37}\text{Na}_{0.14}\text{Pt}_3\text{O}_4$ are discussed below.

3.3. Structure of $\text{Ni}_x\text{Na}_y\text{Pt}_3\text{O}_4$

Neutron powder diffraction experiments on $\text{Ni}_x\text{Na}_y\text{Pt}_3\text{O}_4$ yielded a pattern generally similar to that of $\text{Co}_{0.37}\text{Na}_{0.14}\text{Pt}_3\text{O}_4$. However, the ordering reflections were extremely diffuse, making the data unsuitable for profile analysis. Electron diffraction patterns for $\text{Ni}_x\text{Na}_y\text{Pt}_3\text{O}_4$ confirmed the presence of the ordering reflections. In addition, extra lines from an NiO impurity caused a serious overlap problem with the $321 + 231$ peak. Even allowing for this overlap, a satisfactory structure refinement could not be obtained with these data. Besides having a general similarity with that of $\text{Co}_{0.37}\text{Na}_{0.14}\text{Pt}_3\text{O}_4$ and some degree of ordering on the counterion sites, the structure of $\text{Ni}_x\text{Na}_y\text{Pt}_3\text{O}_4$ must be considered unsolved at the present time.

Electron diffraction patterns of $\text{Ni}_{0.25}\text{Pt}_3\text{O}_4$ crystals from the study of Cahen *et al.* (1972) also contain these ordering reflections. This indicates that the $\text{Ni}_{0.25}\text{Pt}_3\text{O}_4$ structure is analogous to $\text{Co}_{0.37}\text{Na}_{0.14}\text{Pt}_3\text{O}_4$ rather than NaPt_3O_4 or $\text{Li}_{0.64}\text{Pt}_3\text{O}_4$. Electron microprobe analysis confirms that these crystals are Na free. However, the quality of the crystals is too poor to collect single-crystal X-ray diffraction data which would resolve movement of the O atoms from the ideal position at $\frac{1}{4}, \frac{1}{4}, \frac{1}{4}$.

4. Analysis of internal structural deformations

4.1. $\text{Li}_{0.64}\text{Pt}_3\text{O}_4$

Deformations of the ideal NaPt_3O_4 structure that are found in $\text{Li}_{0.64}\text{Pt}_3\text{O}_4$ are displayed in Fig. 3. The displacement of the O atoms off the special position at $\frac{1}{4}, \frac{1}{4}, \frac{1}{4}$ along the threefold axis (the body diagonal of the cubic unit cell) causes the eight-coordinated Li—O polyhedron to distort from a perfect cube to two interpenetrating tetrahedra with Li—O distances of 2.22 and 2.65 Å, respectively. Fig. 3(a) shows these shifts, with four O atoms displaced toward the Li cation (dark bonds) and four displaced away (light bonds). The four O atoms displaced toward the Li cation at 0,0,0 are displaced away from the eight-coordinated Li at $\frac{1}{2}, \frac{1}{2}, \frac{1}{2}$. The O—O distance across the edge of the distorted eightfold coordination polyhedron is 2.83 Å.

The movements of the O atoms also cause deformation of the square-planar PtO_4 groups. In Fig. 3(b), the shifts of the O atoms relative to two Li atoms separated by a unit-cell translation are shown by the arrows. The Pt position is completely constrained by symmetry, so the movements of the O atoms out of the plane of the ideal PtO_4 group cause a minor tetra-

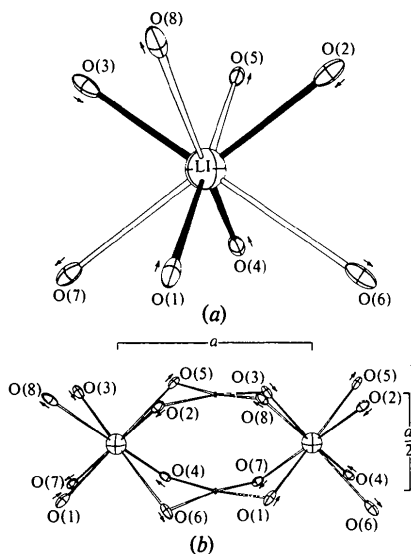


Fig. 3. (a) ORTEP (Johnson, 1965) drawing of eight-coordinated Li in $\text{Li}_{0.64}\text{Pt}_3\text{O}_4$. (b) ORTEP drawing of a portion of the $\text{Li}_{0.64}\text{Pt}_3\text{O}_4$ structure along $[100]$ showing distortion of the PtO_4 groups.

hedral distortion, with an O–Pt–O angle across the diagonal of the square plane of 173° rather than 180° for a perfect square-planar site. The other O–Pt–O angle is 90° . The Pt–O distance for the PtO_4 groups is 2.00 \AA .

Information on thermal motion calculated from anisotropic temperature-factor coefficients of refinement (I), given in Table 2, is consistent with the types of deformations seen in this structure. With O and Li atoms alternately juxtaposed in the $[111]$ direction, the oxygen thermal ellipsoid is elongated along this threefold axis with a root-mean-square (r.m.s.) displacement of 0.15 \AA parallel to $[111]$ and 0.07 \AA in the plane perpendicular to $[111]$, as compared with 0.11 and 0.06 \AA , respectively, for $\text{Na}_{1.0}\text{Pt}_3\text{O}_4$ (Schwartz *et al.*, 1982). The motion of the O atom and the isotropic vibration of the Li atom (r.m.s. displacement = 0.16 \AA) are in response to the presence of a small Li^+ cation in a site normally occupied by much larger ions. The average Li–O distance, 2.44 \AA , is barely shorter than the Na–O distance of 2.46 \AA in NaPt_3O_4 (Schwartz *et al.*, 1982), even though eight-coordinated Li^+ has an ionic radius of 0.92 \AA as compared to 1.18 \AA for eight-coordinated Na^+ (Shannon, 1976). Static positional disorder due to the large number of eight-coordinated vacancies also contributes to the highly anisotropic thermal ellipsoid.

4.2. $\text{Co}_{0.37}\text{Na}_{0.14}\text{Pt}_3\text{O}_4$

The most characteristic feature of the $\text{Co}_{0.37}\text{Na}_{0.14}\text{Pt}_3\text{O}_4$ structure, the symmetrically inde-

pendent eight-coordinated counterion sites at $0,0,0$ and $\frac{1}{2},\frac{1}{2},\frac{1}{2}$, is a direct consequence of cation-vacancy ordering. All eight O atoms at x,x,x collapse toward the counterion (Fig. 4a) and remain on the threefold axis. Since all the O atoms are shifted toward the cation, the perfect cubic nature of the eight-coordinated site is preserved with a metal–oxygen distance of $2.36 (1) \text{ \AA}$. All O–O distances along the edges of the occupied cubic coordination polyhedron are $2.73 (2) \text{ \AA}$. This change in the oxygen position towards the occupied metal site at $0,0,0$ increases the distance, relative to the ideal NaPt_3O_4 structure, between the vacancy at $\frac{1}{2},\frac{1}{2},\frac{1}{2}$ and its eight coordinating O atoms to $2.52 (1) \text{ \AA}$. The O–O distance along the edge of the vacant cubic coordination polyhedron is $2.91 (1) \text{ \AA}$. The relaxation of the oxygen anions toward bonded cation neighbors and away from vacancies is commonly seen in compounds with partially occupied sites (Shannon, 1976).

The platinum position is not completely constrained by symmetry in $\text{Co}_{0.37}\text{Na}_{0.14}\text{Pt}_3\text{O}_4$, and Pt is free to move in a direction perpendicular to the plane of the PtO_4 groups. However, the movement of Pt away from the position it occupies at $\frac{1}{4},0,\frac{1}{2}$ in the NaPt_3O_4 and $\text{Li}_{0.64}\text{Pt}_3\text{O}_4$ structures is small. The Pt–Pt distances are $2.87 (2)$ and $2.77 (2) \text{ \AA}$. There is a slight bowing of the PtO_4 groups away from the vacancies in the structure (Fig. 4b), as the O atoms are displaced toward the occupied cation site. The O–Pt–O angles for the distorted PtO_4 groups are $86.3 (5)^\circ$ for O atoms moving towards each other [e.g. O(4) and O(6)], $93.5 (5)^\circ$ for O atoms moving away from each other [e.g. O(4) and O(7)] and $176 (1)^\circ$ across the diagonal of the square plane [e.g. O(4)–Pt–O(1)]. The Pt–O distance for PtO_4 groups is 1.99 \AA . All bond distances and angles given are based on atom positions obtained

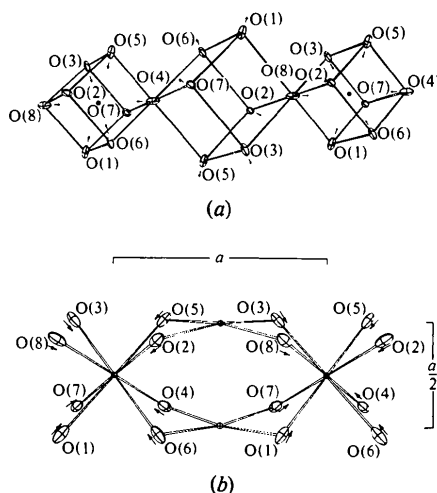


Fig. 4. (a) ORTEP drawing of the $\text{Co}_{0.37}\text{Na}_{0.14}\text{Pt}_3\text{O}_4$ structure along $[111]$. (b) ORTEP drawing of the $\text{Co}_{0.37}\text{Na}_{0.14}\text{Pt}_3\text{O}_4$ structure along $[100]$.

from the *POWLS* refinement at 2.460 Å (column III, Table 3).

Thermal motion for oxygen in $\text{Co}_{0.37}\text{Na}_{0.14}\text{Pt}_3\text{O}_4$ is comparable with that previously described for $\text{Li}_{0.64}\text{Pt}_3\text{O}_4$. The r.m.s. amplitude in the [111] direction is approximately a factor of two larger than that in the plane perpendicular to [111].

5. Discussion

5.1. Crystal chemistry of $\text{Co}_{0.37}\text{Na}_{0.14}\text{Pt}_3\text{O}_4$

The application of chemical constraints, based on atomic absorption analysis for Co and Na, during refinement of scattering lengths for the *A*, *B*, and square-planar sites as described above and given in Table 3, can be used to draw some semi-quantitative conclusions concerning the crystal chemistry of Co in $\text{Co}_{0.37}\text{Na}_{0.14}\text{Pt}_3\text{O}_4$. The marked improvement in discrepancy factors for the refinement where the sum of the scattering lengths of the *A* + *B* sites is not constrained to 3.1 fm per unit cell, the sum of Co + Na scattering, and the square-planar site scattering length is refined rather than constrained at 57 fm per unit cell, the value when the site is fully occupied with platinum, is evidence of counterion occupancy on the platinum site. Since Co^{2+} is known to occur in square-planar coordination and Na^+ is not, it is assumed that the decrease in the scattering length of the square-planar site is due to the substitution of Co^{2+} for Pt^{2+} , as the scattering length of cobalt is $\frac{1}{3}$ that of platinum. It should be noted that the scattering length of platinum is not well known, making quantitative analysis of this system more difficult.

It is not possible to determine uniquely the distribution of cobalt and sodium between the two eight-coordinated sites, so a random distribution is assumed. However, using this crystal-chemical model, the refined site scattering lengths for *A* and *B* suggest the larger *B* site is virtually empty, with a scattering length of 0.1 (4) fm per unit cell, as compared with 1.8 (2) fm per unit cell for the *A* site. The cation distribution obtained from this refinement is $^{\text{VIII}}(\text{Co}_{0.16}\text{Na}_{0.14})^{\text{IV}}(\text{Co}_{0.21}\text{Pt}_{2.79})\text{O}_4$. This distribution is not categorical, but it is considered indicative of multiple occupancy for cobalt in this sample. The unusual nature of eight-coordinated cobalt is reflected in this distribution, with cobalt substituting for platinum in square-planar coordination as well as being present in the normal counterion site.

5.2. Non-stoichiometry and structural considerations

The two types of internal structural deformations of the ideal NaPt_3O_4 structure demonstrated by $\text{Li}_{0.64}\text{Pt}_3\text{O}_4$ and $\text{Co}_{0.37}\text{Na}_{0.14}\text{Pt}_3\text{O}_4$ can be related to the

compositional range found for Li and Co in $M_x\text{Pt}_3\text{O}_4$ compounds. While the Co content has been seen to be restricted to $x \lesssim 0.5$ cations per formula unit, Li compositions over the full range from $0 \leq x \leq 1$ can be synthesized (Shannon *et al.*, 1982). This empirical observation of the chemical behavior of these counterions can now be related to the changes in the eight-coordinated site they promote. The $\text{Li}_{0.64}\text{Pt}_3\text{O}_4$ distortion leaves the *A* and *B* sites symmetrically equivalent, thus posing no structural constraints on the chemistry. However, since Co and Na are ordered in $\text{Co}_{0.37}\text{Na}_{0.14}\text{Pt}_3\text{O}_4$ into one of the two available eight-coordinated sites, and effectively forbidden from entering the other, this imposes a structural limit on substitution at 0.5 cations per formula unit, discounting any square-planar Co that may be present.

The tendency of the eight O atoms to collapse towards the cobalt cation can be understood in terms of crystal-field theory. The cubic crystal-field splitting parameter, Δ_c , can be shown to have approximately twice the value of the tetrahedral crystal-field splitting parameter, Δ_t (Burns, 1971). This means that for transition metals with a high-spin d^7 configuration (*e.g.* Co^{2+}) a cubic crystal field will always result in a lower energy state than a tetrahedral crystal field. Therefore, the collapse of the cubic counterion site in $\text{Co}_{0.37}\text{Na}_{0.14}\text{Pt}_3\text{O}_4$ is energetically preferable to the tetrahedral distortion seen in $\text{Li}_{0.64}\text{Pt}_3\text{O}_4$.

Bond distances for PtO_4 groups and for metal-oxygen eight-coordinated polyhedra show that though the oxygen positions are displaced from the ideal towards the small Li and Co counterions, the Pt—O bond is not significantly affected by this movement. Based on known ionic radii for Li and Co in eight-coordination in oxides (Shannon, 1976), Li—O and Co—O distances would be expected to be < 2.3 Å when in fact they are significantly larger in the present compounds. The Pt—O distances, 2.00 Å in both $\text{Li}_{0.64}\text{Pt}_3\text{O}_4$ and $\text{Co}_{0.37}\text{Na}_{0.14}\text{Pt}_3\text{O}_4$, are close to the predicted value based on an ionic radius of 0.60 Å for square-planar platinum.

For cobalt, the cubic site in $\text{Co}_{0.37}\text{Na}_{0.14}\text{Pt}_3\text{O}_4$ is probably unique. In the $[\text{Co}(\text{NO}_3)_4]^{2-}$ moiety, the first known example of eight-coordinated cobalt (Bergman & Cotton, 1966), the coordination polyhedron is a dodecahedron, consisting of two interpenetrating bisphenoids (tetrahedra distorted to D_{2d} symmetry). This configuration is more stable than the cube, based on ligand-ligand repulsion (Hoard & Silverton, 1963; Kepert, 1965), indicating the control platinum has in preventing more dramatic changes in the counterion coordination polyhedron that would result in a more energetically stable oxygen configuration.

5.3. Conclusions

Some important features of the structure of non-stoichiometric $M_x\text{Pt}_3\text{O}_4$ compounds with relatively

small counterions have been elucidated. Magnetic-susceptibility measurements on $\text{Co}_{0.37}\text{Na}_{0.14}\text{Pt}_3\text{O}_4$ (Schwartz & Parise, 1982) yield evidence that the cobalt present is in the divalent state and is consistent with the model suggested of multiple site occupancy for cobalt.

The details of the $\text{Ni}_x\text{Pt}_3\text{O}_4$ structure are still problematic. Ordering reflections in both $\text{Ni}_{0.25}\text{Pt}_3\text{O}_4$ and $\text{Ni}_x\text{Na}_y\text{Pt}_3\text{O}_4$ suggest a situation similar to that described above for $\text{Co}_{0.37}\text{Na}_{0.14}\text{Pt}_3\text{O}_4$. The poor quality of diffraction data collected suggests $\text{Ni}_{0.25}\text{Pt}_3\text{O}_4$ and $\text{Ni}_x\text{Na}_y\text{Pt}_3\text{O}_4$ are poorly crystallized compounds. This may be related to the extremely small size of Ni relative to other cations found in the $M_x\text{Pt}_3\text{O}_4$ structural family. These compositions remain an outstanding problem within the $M_x\text{Pt}_3\text{O}_4$ series.

We would like to thank D. E. Cox for his most generous and invaluable contributions of time, effort and expertise throughout this entire project, C. M. Foris for assistance with the Guinier photographs, B. F. Burgess and C. R. Perrotto for atomic absorption analyses. L. M. Corliss and J. M. Hastings of Brookhaven National Laboratory collected neutron powder diffraction data at $\lambda = 1.343 \text{ \AA}$ for all samples. The work was performed under NSF Grant DMR79-06900 and at the Experimental Station of E.I. du Pont de Nemours and Company.

References

- BACON, G. E. (1978). Brookhaven National Laboratory compilation (unpublished).
 BERGMAN, J. G. & COTTON, F. A. (1966). *Inorg. Chem.* **5**, 1208–1213.
 BERGNER, V. D. & KOHLHAAS, R. (1973). *Z. Anorg. Allg. Chem.* **401**, 15–20.

- BURDETT, J. K., HOFFMANN, R. & FAY, R. C. (1978). *Inorg. Chem.* **17**, 2553–2568.
 BURNS, R. G. (1971). In *Mineralogical Applications of Crystal Field Theory*. Cambridge Univ. Press.
 CAHEN, D., IBERS, J. A. & MUELLER, M. H. (1974). *Inorg. Chem.* **13**, 110–115.
 CAHEN, D., IBERS, J. A. & SHANNON, R. D. (1972). *Inorg. Chem.* **11**, 2311–2315.
 CAHEN, D., IBERS, J. A. & WAGNER, J. B. (1974). *Inorg. Chem.* **13**, 1377–1388.
 HEWAT, A. E. (1973). UK Atomic Energy Authority Research Group Report RLL 73/897 (unpublished).
 HEWAT, A. E. (1979). *Acta Cryst.* **A35**, 248.
 HOARD, J. L. & SILVERTON, J. V. (1963). *Inorg. Chem.* **2**, 235–243.
 JOHNSON, C. K. (1965). *ORTEP*. Report ORNL-3794. Oak Ridge National Laboratory, Tennessee.
 KEPERT, D. L. (1965). *J. Chem. Soc.* pp. 4736–4744.
 KOESTER, L. (1977). *Springer Tracts Mod. Phys.* **80**, 1–55.
 LAZAREV, V. B. & SHAPLYGIN, I. S. (1978a). *Russ. J. Inorg. Chem.* **23**, 163–170.
 LAZAREV, V. B. & SHAPLYGIN, I. S. (1978b). *Russ. J. Inorg. Chem.* **23**, 1610–1612.
 LAZAREV, V. B. & SHAPLYGIN, I. S. (1978c). *Mater. Res. Bull.* **13**, 229–235.
 RIETVELD, H. M. (1969a). Reactor Centrum Nederland Research Report RCN 104 (unpublished).
 RIETVELD, H. M. (1969b). *J. Appl. Cryst.* **2**, 65–71.
 SCHWARTZ, K. B. & PARISE, J. B. (1982). *J. Phys. Chem. Solids*. In the press.
 SCHWARTZ, K. B., PREWITT, C. T., SHANNON, R. D., CORLISS, L. M., HASTINGS, J. M. & CHAMBERLAND, B. L. (1982). *Acta Cryst.* **B38**, 363–368.
 SHANNON, R. D. (1976). *Acta Cryst.* **A32**, 751–767.
 SHANNON, R. D., GIER, T. E., CARCIA, P. F., BIERSTEDT, P. E., FLIPPEN, R. B. & VEGA, A. J. (1982). *Inorg. Chem.* In the press.
 WASER, J. & McCLANAHAN, E. D. (1951). *J. Chem. Phys.* **19**, 413–416.
 WILL, G. (1979). *J. Appl. Cryst.* **12**, 483–485.

Acta Cryst. (1982). **B38**, 2116–2120

Deformation Density in Complex Anions.

III.* Potassium Perchlorate

BY J. W. BATS AND H. FUESS

*Institut für Kristallographie und Mineralogie der Universität Frankfurt, Senckenberganlage 30,
 Postfach 11 19 32, 6000 Frankfurt am Main 11, Federal Republic of Germany*

(Received 1 December 1981; accepted 3 March 1982)

Abstract

KClO_4 , space group $Pnma$, $Z = 4$, $a = 8.765(1)$, $b = 5.620(1)$, $c = 7.205(1) \text{ \AA}$, $V = 354.9(1) \text{ \AA}^3$ at 120 K.

* Part II: Fuess, Bats, Dannöhl, Meyer & Schweig (1982).

Neutron diffraction: ω scan, $\lambda = 1.0272(5) \text{ \AA}$, 831 independent reflections, $(\sin \theta/\lambda)_{\max} = 0.80 \text{ \AA}^{-1}$, $R_w(F) = 0.022$. X-ray diffraction: $\omega-2\theta$ scan, Mo $K\alpha$ radiation, two crystals: (I) 1884 reflections, $(\sin \theta/\lambda)_{\max} = 1.08 \text{ \AA}^{-1}$, $R_w(F) = 0.030$; (II) 1153 reflections,